Dynamics of leaf area for climate and weather models

Robert E. Dickinson,[1] Yuhong Tian,[2] Qing Liu,[1] and Liming Zhou[1]

[1] Leaf area is the most relevant scalar variable for describing the dynamics of vegetation on seasonal time scales, and hence is required as part of the land-surface component of a meteorological model. A mathematical scheme for the dynamic vegetation component of such a model is formulated and reduced to a toy model for seasonal leaf dynamics. Leaf growth is seen as a temperature-initiated instability of the ecosystem that drives it away from its state of winter dormancy; the onset of dormancy in autumn consists of cold temperatures breaking the summer-time attractor; the temperature-dependent controls are represented by a "ramp-up" function. Results from ensemble simulations driven by a stochastic temperature model show that leaf variability statistics have a very strong seasonality, such that variability is largely confined to spring and autumn. These variability windows promote non-Gaussian and nonstationary statistics that occur when the stable attractor of one season has flipped to the stable attractor of the other season. During such periods of high variability, any dynamic vegetation model will be most unreliable without observational constraints because of its unstable trajectory.

1. Introduction: What is Needed?

[2] Terrestrial ecosystems have significant interactions with the physical climate system. These interactions occur through many parameters and on multiple time scales, determining the hydrological and thermal aspects of surface and near surface climate for days out to seasons [e.g., *Fitzjarrald et al.*, 2001; *Levis and Bonan*, 2004; *Friend and Kiang*, 2005]. On interannual time scales, the seasonal statistics of this coupling plus biogeochemical processes determine the longer time scale evolution of plant canopy properties such as the leaf cover during the peak growing season, resulting from the changing competitive status for light, water, and nutrients, and hence shifts in species and plant functional type composition and in the net ecosystem storage of carbon [e.g., *Fung et al.*, 2005].

[3] The longer time scale changes of the terrestrial biosphere have been addressed with models that change carbon storage and plant functional types [e.g., by *Foley et al.*, 1998; *Bonan et al.*, 2003; *Arora and Boer*, 2006]. A major state variable of such models on all time scales is the leaf area index (LAI). This term has been described by empirical phenology rules relating the LAI to temperature [e.g., *Prentice et al.*, 1992; *Foley et al.*, 1996; *Levis and Bonan*, 2004; *Kim and Wang*, 2005; *Arora and Boer*, 2005].

[4] The modeling of the dynamics of leaf area on the seasonal and shorter time scales, the thrust of this paper, has been less addressed, and has consisted of two distinct

directions: (1) processes models [*Dickinson et al.*, 1998, 2002], intended to simulate variability of LAI on shorter time scales and (2) remote sensing modeling that uses quantitative satellite imagery to infer canopy properties, in particular, leaf area, albedo, fractional cover, and plant functional types [e.g., *Knyazikhin et al.*, 1998; *Schaaf et al.*, 2002; *DeFries et al.*, 1999; *Friedl et al.*, 2002]. Simple process concepts have been used to constrain such data, e.g., the observational inference of phenology [e.g., *Justice et al.*, 1985; *Kaduk and Heimann*, 1996; *Botta et al.*, 2000; *Zhang et al.*, 2003; *Ahl et al.*, 2006], and the filling of holes for missing data which is based on the concept of the continuity/correlation between canopy properties at different pixels and at different times [e.g., *Moody et al.*, 2005].

[5] Linear regression correlations for the onset of spring growth have commonly used accumulated degree days. For individual species, this approach improves by a few days upon a simple day of the year climatological relationship [e.g., *Hunter and Lechowicz*, 1992; *Richardson et al.*, 2006]. Some such temperature related phenology models have been tested for assimilation of leaf area [e.g., *Koetz et al.*, 2005]. However, the use of such degree day estimates by dynamic vegetation models may produce timing errors as large as 6 weeks [*Kucharik et al.*, 2006] unless correlated to additional parameters such as midwinter or annual mean temperatures [*White et al.*, 1997; *Zhang et al.*, 2004; *Kathuroju et al.*, 2007]. Because various stress terms and the range of LAI can be scaled from 0 to 1, hyperbolic tangent (i.e., "logistic") functions may provide better fitting than a linear function [e.g., *Leinonen*, 1996; *Chuine*, 2000] for the construction of a dynamic model.

[6] Plants can also depend on photoperiod (i.e., length of day) signals for initiation or termination of various phenological stages as can be established from growth chamber

[1] School of Earth and Atmospheric Sciences, Georgia Institute of Technology, Atlanta, Georgia, USA.
[2] IMSG at NOAA NESDIS STAR, Camp Springs, Maryland, USA.

data, e.g., as modeled by *Yan and Wallace* [1998]. The photoperiod of natural vegetation is entirely controlled by latitude and day of the year. *Fisher et al.* [2007] used 6 years of MODIS data to determine patterns of greenness over New England and found that a photoperiod model (equivalent to climatological average) was as accurate as a degree-day model in establishing the onset of greenness (both with RMS error of 6.6 days).

[7]   The present paper develops an approach to modeling the time evolution of leaf area for use in a meteorological model and with a dynamical response to meteorological drivers. It is not intended to describe directly biological processes or phenological data but rather to simply represent the meteorological dependences of leaf area including especially its time scales of adjustment. This model is formulated as a differential equation that can take a time series of noisy data on leaf-area and establish a smooth curve in time through the latter. Such smoothing is founded on a priori information captured by the dynamical model. For such modeling, it is convenient to take leaf area as a stochastic variable, i.e., one with random statistics varying in time. This is a mathematical, not a physical assumption about the nature of the leaves so treated.

[8]   An overarching intent of the modeling described here is to provide a framework for the assimilation of global satellite data. Such assimilation requires a dynamic model for the controls on the variation of leaf area that can be integrated as part of a meteorological model and that uses data available to such a model for assimilation of measured information related to leaf area. For such applications, it is not as important that what equations to use as the applicability of the dynamical model. The details of this application are presented in another paper [*Liu et al.*, 2008]. The explicit intent of this study is not to generate a particular set of model parameters or particular leaf area climatology but rather to provide a model structure that depends on parameters whose values can be efficiently determined by the appropriate data assimilation procedures.

[9]   Section 2 describes the mathematical framework in which leaf area becomes part of a meteorological model through its connections to climate and hydrological variables and introduces the idea of a "toy" model of this system to better illustrate the components of this coupling most related to the dynamics of leaf area. It also describes how temperature variability is generated that is used to force the model. Section 3 describes the details of the toy model with an example of a cold-limited Northern deciduous forest. Section 4 describes the climatological statistics of this toy model, followed by sections 5 and 6 of discussion and conclusions.

2.   Dynamical System Approach to Coupling Between the Physical Climate System, Ecosystems, and Hydrology

[10]   Current meteorological models, as used for climate and weather simulations, provide complicated time-dependent systems of differential equations for the climatological and hydrological states of the system. The climate and hydrology state variables of these equations can formally be denoted T and W. Some versions of such models also include equations for dynamic vegetation Let L be a vector state variable

representing all the components of such that dynamically couple to the climate and hydrological systems. The evolution of L in a meteorological model is, in principal, provided by the vector differential equation:

$$dL/dt = G(L, T, W) - S(L, T, W) \qquad (1)$$

where t is time, and G and S denote a vector valued functions respectively for the gain (or growth) of L and its stress (i.e., loss). The required functions will include many parameters, including external forcing terms such as the solar radiation incident at the top of the atmosphere and aspects of soil and atmospheric composition whose change is not part of the modeling. A primary motivation for this paper has been the mismatch between what is used for equation (1), if anything, in current meteorological models and what appears to be required for the successful assimilation of information on leaf area.

[11]   For this toy model, we assume that all the variability of the ecosystem can be projected onto the leaf area index which is denoted L, that all the climate variability can be described by a temperature T, and that all of the hydrological variability by a soil stress water parameter W. Thus we reduce the dimensionality of our system from very large to the 3 state variables (L, T, W). This paper treats all these variables as random, as this provides a useful mathematical framework for characterizing their statistical properties. The definition of this time evolving state requires some geographical description of what spatial averaging is intended. In particular, the model could apply globally, as an average over a region, or at a local site.

[12]   The water stress parameter W will depend mostly or entirely on the profile of soil moisture. Leaves undergo moisture stress when they cannot fully respond to the atmospheric and radiative driven demand, i.e., the "potential" evapotranspiration. Thus moisture stress can be scaled to the ratio of actual evapotranspiration to potential evapotranspiration which can be related to W.

[13]   Recent phenological studies of semi-arid systems provide a good observational basis for prescribing the needed water stress parameters. *Jolly and Running* [2004] address the seasonal dynamics of L for a savanna and a woodland pft in the Kalahari region of southern Africa. They compared observations from AVHRR with L modeled with a version of the BIOME-BGC ecosystem model that was modified to turn on its productivity after adequate precipitation. They used hydrological budgeting arguments to determine the initiation of leaf-growth and the loss of leaves from water stress but did not include a coupled dynamical model for soil moisture. *Zhang et al.* [2005] examined the "NBAR EVI" product from MODIS. They characterized the phenology of three regions of Africa, including the sub-Saharan zone down to 5 N. Both studies indicate no extended plateau periods of maximum greenness, although this inference may be an artifact of the fitting to low-temporal resolution data. *Zhang et al.* [2005] show extended periods of minimum leaf northward of 10N. They found that the integral of seasonal precipitation provided a good indicator of the onset of green-up, and days since the end of the rainy season as an indicator of the probability of the onset of dormancy.

[14] The conclusions of these papers involve water-stress driven phenologies and so their derivation would requires additional consideration of hydrological inputs to the models. In order to analyze the simplest example of equation (1), this paper only addresses further (in section 3) a cold-stress formulation depending on coupling to a variable temperature.

[15] As explained above, the climate state is assumed to be adequately described by a simple scalar temperature T that represents a distribution of values. The present study uses this term only to generate variability of the ecosystem state variable L. The most realistic inclusion of temperature might be through particular observations at some site. This form of forcing is not used here for two reasons: (1) the model for L is intended to be driven by temperatures provided by a meteorological model, not observed values; (2) perhaps more importantly, we want to establish explicitly how and in what form the climatological statistics of L are established, given a statistical model of T.

[16] The variability of temperature is represented by a seasonal cycle, a stochastic term, and an adjustment term for the effect of the diurnal cycle, i.e.:

$$T = T_a + T' + T_d, \qquad (2)$$

where T_a is an annual cycle of temperature, e.g., as prescribed by using linear interpolation between monthly mean values or by expanding monthly means in a Fourier series with annual periodicity, T' is a stochastic term and T_d is an adjustment term for a diurnal cycle contribution with constant amplitude, i.e., it is the diurnal cycle contribution at some time of a day. How the latter term contributes to leaf change does not appear to be established.

[17] We hypothesize that daytime maximum T contributes to initial leaf growth and that nighttime minimum T affects the development of leaf senescence or frost damage as cold stress develops. Empirical studies of phenology have for convenience used meteorological station data to infer a driving temperature. We follow such a practice in this paper, but recognize that the leaf development phenology is likely more closely linked to leaf and soil temperature, as may be estimated by satellite radiometric skin temperature [e.g., as used by *Zhang et al.*, 2004]. We mimic the possibility of a seasonally changing contribution of the diurnal temperature to leaf dynamics by adjusting T by $T_d = 5$ K cos[$(2\pi(t - 140)/365$]. The 5 K is the amplitude of the diurnal cycle, but the cosine term provides an annual periodicity. Together, these two factors provide near the maximum positive bias contribution in the spring and negative in the fall. The approach might be equally effective with this term being left out given that observed daytime average temperatures are constituted from the daily maximum and minimum values and are highly correlated with them. It illustrates the hypothetical but plausible possibility that daily maximum temperatures are needed for leaf growth in spring and daily minimum values for senescence or frost damage in the fall. Inclusion of an actual diurnal cycle would introduce rapid but largely reversible changes. The T_d as formulated will contribute more irreversible effects of daily temperature extremes.

[18] The stochastic term T' is what is left over after seasonal and diurnal cycles are removed. The statistics of this term can be approximated by a Gaussian distribution with memory of past weather disturbances. It can be and is modeled by:

$$dT'/dt + (T' - f \cdot \delta T)/\tau = 0 \qquad (3)$$

where f is chosen from a random Gaussian distribution of unit variance at a daily frequency (that is also taken as the interval of the differencing of equation (3) for numerical solution), τ is the temporal autocorrelation time, taken to be 6 days, as suggested by *Shukla and Kinter* [2006], and δT is a prescribed scale of temperature variability in K taken to be $\delta T = 16 - 10\sin(t \cdot \pi/365.0)$.

[19] The random f term provides the variability contributed by daily weather disturbances. Without it, the T' would decay to zero with time scale τ. The factor δT is designed to represent the daily RMS variability that would occur from the random forcing in the absence of temporal auto-correlation. Its half-sine seasonal variation fits the lower variability experienced in summer. Daily variability corresponds approximately to the averaging of τ such samples and is reduced from δT by a factor of about 0.3 whereas monthly variability is reduced by a factor of about 0.18. Winter variability is larger than summer in the extratropics by about a factor of 2. Allowing for this difference in equation (3) makes the statistics "cyclo-stationary" rather than stationary.

[20] Equation (3) is, in practice, no more than a simple stochastic "weather generator" intended to adequately provide the most essential variability of L that might otherwise be obtained from a much more elaborate climate model. The technical difficulties arising in the numerical integration of white noise forcing [e.g., as discussed by *Ewald et al.*, 2004] are avoided by assuming that the temperature variability varies smoothly between the daily samples. Equation (3) is instead a shortcut to avoid for the paper the complication of running an actual weather model, the intended driver of the leaf area model.

[21] Equation (3) was evaluated using an ensemble of 10,000 members. An annual temperature T_a is obtained from 35 years of observed daily temperatures at a meteorological station close to Harvard Forest [*Williams et al.*, 2006]. Initiation of leaf growth at this site is only temperature limited [*Jolly et al.*, 2005].

3. The Ecosystem State Model L as a Dynamic Leaf

[22] A scalar version of equation (1) for L is written similarly to equation (3) as:

$$dL/dt + \lambda(L, T, W)L = 0 \qquad (4)$$

[23] The term λ is the inverse of the time scales on which L grows (negative λ) or decays (positive λ). It is simply obtained from the G of equation (1) by dividing this term by L. As was assumed for G, it has a nonlinear dependence on the state variables T, W, and L.

[24] Although not indicated in equation (4), it should also have a small photosynthate forcing term that is only relevant when L is small. The effect of such a term is implemented in the code by taking $L = $ max (L, ε), with $\varepsilon = 0.01$. This

term is necessary for biological and mathematical reasons. Biologically, at the initiation of budburst, stored photosynthate is necessary to provide growth as there are no leaves to accumulate carbon. Mathematically, the solution of equation (4) at $L = 0$ is at a point of unstable equilibrium and will remain there until some mechanism is provided to push it away from 0. Smaller values than used were found to noticeably retard the springtime growth.

[25] Equation (4) is used as a forecast model, i.e., only the past is known [e.g., *White and Nemani*, 2006]. Because we have assumed no direct stochastic forcing in equation (4), the variability of L is controlled entirely by that of T and W and so L will remain within reasonable values if the controlling relationships are reasonable. The stochastic forcing is multiplicative and included indirectly through the nonlinear dependence of λ on T and W.

[26] The term λ, obtained from the scalar version of $\boldsymbol{G}$ in equation (1) by dividing it by L, similarly divides into gain $(-\lambda_G)$ and stress (λ_S) terms. Positive terms λ_S will represent the loss of L to predictable respiration and stresses, e.g., as depending on temperature and water, while negative terms $-\lambda_G$ represent the contribution to leaf growth of the predictable physiology of carbon assimilation.

[27] The stress component of λ_S is parameterized as

$$\lambda_S = \lambda_0\{1. + a[1. - R(x)] + b[1 - R(y)]\}, \qquad (5)$$

where λ_0 ($\lambda_0 = 0.05$ day^{-1}) is an inverse time scale characterizing normal respiration losses balancing normal growth at steady state, a, b express enhanced loss from stress terms, $R(x)$ is a smooth version of Heaviside "ramp-up" function, with the latter going from near 0 at $x < -1$ to 1 at $x \geq 1$. We assume that $R(x) = 0.5\,(1. + \tanh(x)) = 1./(1. + \exp(-2x))$, a basis function commonly used for various non-linear statistical fitting techniques. The term x is the normalized range of temperatures over which cold stress switches off and y is the range of W over which water stress switches off. For initial investigation, we have taken b = 0, i.e., have omitted the water stress term; $x = (T - T_{min})/\Delta T$, where $\Delta T = 5$, $T_{min} = 5°C$, and $a = 9$. These numerical values are guesses that were derived from time scale estimation and limited testing. They are not given as recommended values but as explanation for what was used to generate subsequent figures, and have been easily modified by optimization to data, a step not described here to limit the complications of the paper.

[28] The growth component $-\lambda_G$ is parameterized as

$$\lambda_G = \lambda_0 R(x)(L_0/L)[1. - \exp(-cL)]. \qquad (6)$$

[29] At small L equation (6) gives growth linear in L but at large L the growth rate approaches the constant $\lambda_0 L_0$ ($L_0 = 5.$) representing light limited growth. If the term $[1.-\exp(-cL)]$ is expanded by Taylor's series to two terms in L, it would form the logistic differential equation more familiar to biologists, with stable equilibrium point $L = 2/c$. The $[1.-\exp(-cL)]$ dependence on L mimics a dependence on light attenuation, e.g., PAR absorbed by sunlit leaf area. It has commonly been used in simple nonlinear modeling of vegetation dynamics (e.g., *Zeng et al.* [2005]) for past references and a consideration of alternative such

"ramp-up" functions). The numerical value of c, has been taken to be 1.0. It affects the degree to which light saturation depends on L and, growth at small L is proportional to it.

[30] With the use of the "sigmoid" temperature dependence of λ in equations (4)–(6), the leaf trajectory has a stable limit point at $L = 0$ at cold temperatures, until λ changes sign with warmer temperatures at some temperature threshold T_0. The commonly used accumulation models for phenological onset are used to trigger a "green-up" phase of leaf growth. Over the steep central part of the sigmoid, λ is linearly proportional to T, so its integration for $\log L = \int \lambda dt = \int T dt$, initially accumulates degree days, after temperature exceeds some minimum value. Some studies, e.g., by *Chuine* [2000], have assumed "sigmoidal" rather than linear dependence on T for the accumulation statistic, an algorithm even closer to that of equations (4)–(6). *Jolly et al.* [2005] use an index for beginning of growth derived from a temperature ramp, smoothed over a 21-day running average, which also closely resembles the results of equations (4)–(6). The integration of λ is not determining a threshold, but rather increasing the exponential growth rate of L. After accumulation of about 100 degree days, $-\lambda$ has been increased to λ_0, large enough to initiate growth. Degree days are defined as accumulation of the excess of T over $T_{min} = 5°C$. More degree days are needed when the growing season starts at the steepest part of the annual temperature cycle, as the interval over which λ is linearly proportional to T is more quickly exceeded, and its accumulated growth rate consequently reduced.

[31] The ramp-up functions and associated constants are intended to incorporate the general knowledge of how phenology depends on temperature T and soil water W. Such ramp-up functions are characterized by a width scales and a number of other shape parameters. These parameters would be expected to differ between the two stress terms and the growth term. However, by initially using a fixed shape and the same terms for all 3 components, we reduce the dimensionality without seriously altering the system dynamics. Equations (5) and (6) so constrained, only capture the strongest such functional relationships between L, T, and W. However, because all the biochemical kinetics of plant growth and respiration also depend on T, many other weaker dependences are recognized in process level models. The scaling of such dependence to ecosystems, especially that of respiration, can be somewhat controversial. Further details could be warranted in the context of fitting to good data.

[32] The derivatives of λ with respect to L and T approximate the factors relating variability of λ to that of L and T. The L derivative is needed in the next section:

$$\mu(L) = \partial\lambda/\partial L = R(x)(\lambda_0 L_0)[1. - (1 + cL)\exp(-cL)]/L^2 \quad (7)$$

[33] The trajectories of the ensemble of T simulations as described in the previous section are used to generate an ensemble of L simulations. For plotting purposes, ensemble members within small ranges of L or λ are binned to provide distributional statistics. Figures 1 and 2 provide different perspectives on the resulting seasonally varying probability density function (pdf) of L and λ. Figure 1a shows for each day the boundaries for the smallest and
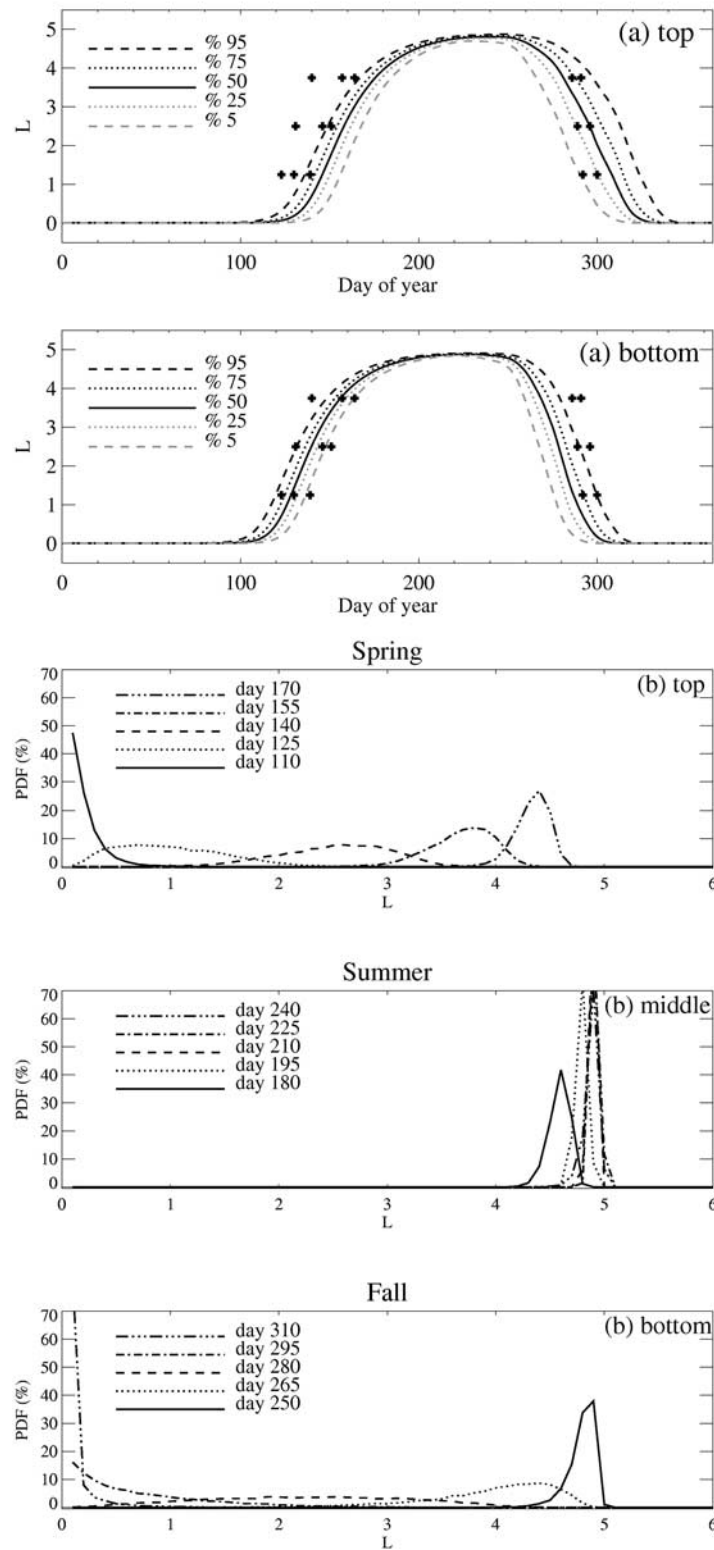
Figure 1. The distribution of leaf trajectories. (a) Percentile boundaries forced by the stochastically generated T (top) without and (bottom) with the inclusion of the diurnal term T_d that provide daytime maximum in spring and nighttime minimum temperature in fall. Three years Harvard Forest data are also plotted as "plus" from *White et al.* [1997] for comparison. (b) The leaf pdf at various times of year, defined as the % of samples in each 0.1 interval of L.
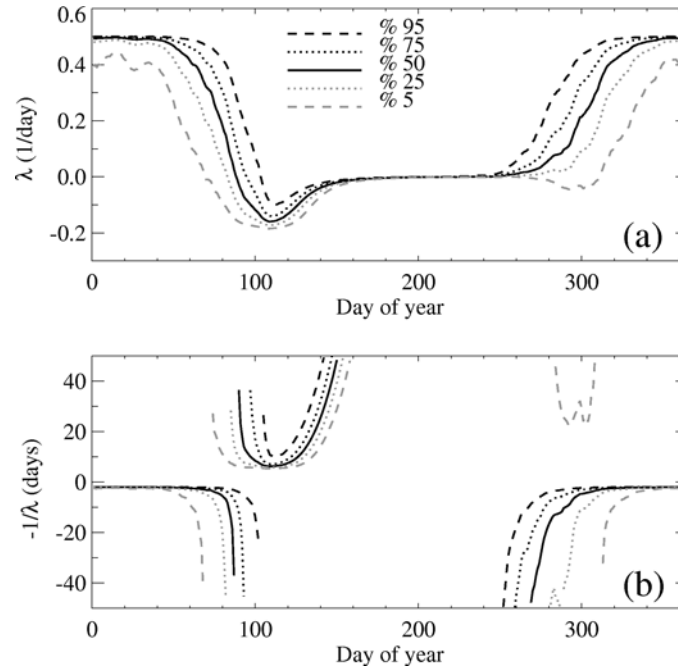
Figure 2. The seasonal variation of the distribution of (a) λ in day^{-1} and (b) $-1/\lambda$ in days showing the periods of stability and instability (positive or negative values of λ).

largest 5% of the L trajectories, the smallest and largest 25% and the median. The variability of these trajectories is controlled by the modeled temperature variability. When the effect of the diurnal cycle (T_d) is considered, the L seasonality apparently is better characterized in spring. Although a given trajectory will show substantial variability on a weekly time scale, these percentile statistics have smooth annual cycles. Figure 1b shows the shape of the pdfs at given times. The major points seen are that the pdfs are narrowly peaked in summer and winter about their climatological values, whereas in spring and fall, they can be much wider, i.e., cover the whole range of possible values of L. Furthermore, the pdf can be strongly positively skewed in early spring or late fall, and negatively skewed in later spring or early autumn. The pdfs of λ have similar asymmetries as illustrated in Figure 2a. The growth time scale of L ($-1/\lambda$) is shown in Figure 2b. The peak rate of growth occurs around day 110–115, corresponding to the time of "budburst" seen in Figure 1, i.e., L growing up to a value of about 0.5. In the autumn, the positive region of the 5% boundary suggests that some of the time, the dynamic leaf, after a large loss, can start to grow before being permanently lost to cold.

4. Climatological Statistics of the Dynamic Leaf

[34] A common observational approach to describing the statistics of the leaf dynamics would be an average over as many years as possible from available data. A common theoretical approach might be to look at equilibrium statistics, i.e., what leaf area is determined by a balance between carbon gains and losses. Because of the nonlinear and dynamical nature of the trajectory of leaves, with the resulting nonstationary and non-Gaussian statistics, any such averaging or equilibrium description would be an

inadequate characterization of what is important about the statistical distributions of the leaf trajectories. The purpose of this section is to improve on the average or equilibrium viewpoints to provide an adequate statistical characterization of the leaf dynamics in terms of dependence on model parameters, including statistics of the temperature forcing and to show a graphical representation of the leaf distributional statistics. We establish in particular, how the average time behavior of the leaves depend on correlation statistics. This is a common result for description of meteorological statistics but apparently has not been previously presented as a characteristic of dynamic vegetation.

[35] The solutions to equation (4) as a nonlinear dynamic equation consist of its climatological average $L_c = \langle L \rangle$ (i.e., an ensemble average over many realizations, denoted "$\langle\ \rangle$" which is assumed to estimate a many year average) and L', the departure in any realization from the climatological value, $L' = L - \langle L \rangle$. The climatological average of a climate state variable such as L_c depends on various higher orders statistics. What statistical information determines the seasonally varying L_c is now established.

[36] The term L_c can be written as:

$$L_c = L_e(T_c) + L^*(T_c) \tag{8}$$

where $L_e(T_c)$ is the equilibrium obtained from equation (4) with the climatological temperature but without the dL/dt term. The term L^* is the additional term added to L_e resulting from the transient time derivative term with only a climatological annual cycle forcing and a contribution from the stochastic variability of T about its climatological values. It is set to 0 in winter when L is at its prescribed minimum value. Quantitatively, L_e is the stable solution of the nonlinear equation $L_e \lambda(L_e, T_c) = 0$ and hence the stable attractor of equation (4). For the cold time of the year,

$L = L_e = 0$ is the only stable solution, whereas in the warm season, $L_e = 0$ is unstable and there is at least one root of $\lambda(L) = 0$ that is stable, i.e., to which equation (4) would converge if T were not changing in time.

[37] The two terms in equation (8) are determined as follows: a) The equilibrium value $L_e(T_c)$ is the solution to the nonlinear equation

$$L_e\lambda(L_e) = 0. \tag{9}$$

[38] For sufficiently large L_e, its root is approximated by:

$$L_e = L_e^0 = R L_0/[1. + a(1. - R)]. \tag{10}$$

[39] This approximation will be accurate to 3 decimal places when $L_e^0 \geq 7$. Otherwise, L_e is determined by iteration from:

$$L_e^{m+1} = L_e^m - \frac{L_e^m \lambda(L_e^m)}{\lambda(L_e^m) + L_e^m d\lambda/dL}, \tag{11}$$

where L_e^m is the mth estimate of L_e, and $d\lambda/dL$ is obtained from equation (7), evaluated at $L = L_e^m$.

[40] At a small enough values of L_e^0, the estimate of equation (11) will not converge, and the only accessible solution is $L_e = 0$. To apply a uniform rule, we iterate equation (11) 10 times and consider the iteration to have converged if the relative change from the 9th to 10th iteration is $\leq 5\%$.

[41] b) The equation for L^*, i.e., the ensemble average departure of L from L_e, is obtained by substituting equation (8) into equation (4) and taking an ensemble average, i.e.:

$$\frac{dL^*}{dt} + \lambda_c L_c = -F, \tag{12}$$

where the change of L^* is forced by the rate of change of the equilibrium solution plus the covariance between L' and λ':

$$F = \langle \lambda' L' \rangle + \frac{dL_e}{dt}. \tag{13}$$

[42] For the region of parameter space that $L^* \ll L_e$, λ^* ($\lambda^* = \lambda_c - \lambda_e$, $\lambda_e = \lambda(L_e)$) can be expanded as $\lambda^* = \mu_e L^*$, the term quadratic in L^{*2} dropped, and equation (12) can be approximated by

$$\frac{dL^*}{dt} + (\mu_e L_e + \lambda_e)L^* = -F. \tag{14}$$

[43] Equations (12) to (14) show how the stochastic variability of λ and hence L will contribute to the climatological average of L. However, they do not suggest what will determine the magnitude of the covariance $\langle \lambda' L' \rangle$. For that, it is useful to use the linearized equation for L', i.e.

$$\frac{dL'}{dt} + \lambda_c L' + L_c \lambda' = 0. \tag{15}$$

[44] Equation (15) is multiplied by L' and averaged over its ensemble, giving

$$\langle \lambda' L' \rangle = -\frac{\lambda_c \langle L'^2 \rangle + \frac{d\langle L'^2/2 \rangle}{dt}}{L_c} = -(\text{term1} + \text{term2}) \tag{16}$$
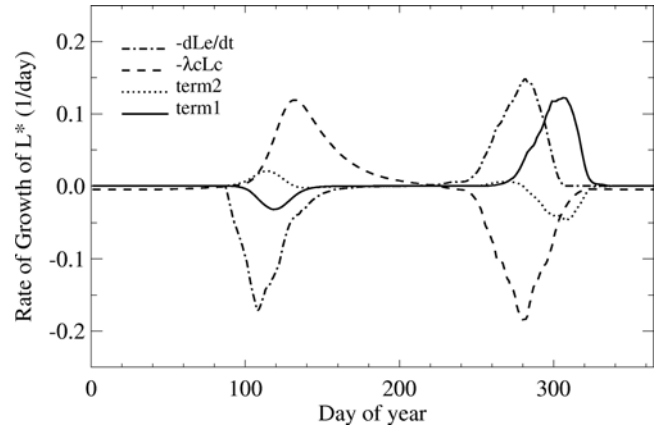

Figure 3. The seasonal variation of the two contributions to covariance $\langle \lambda' L' \rangle$ as defined in equation (16), term1 and term2, positive for contribution to growth, in units of day^{-1}, and compared to the other two forcing terms in equation (12).

[45] Term1 in equation (16) shows how the variance of L contributes to this correlation. It will be negative in the spring when negative λ_c dominates but can take positive values in the fall when positive λ_c dominates. Term2 contributes because of the cyclo-stationarity of the L statistics, i.e., the maximum variability of L in spring and fall. It is consequently of a dipole nature with positive values at the beginning of the spring ramp-up and fall ramp-down and negative values at the end of spring and fall. However, its values at end of spring and beginning of fall are negligible because of the large L_c in the denominator. For either term, positive values promote growth of L^* whereas negative values a decline. The values of these terms are compared to the other terms in equation (12) contributing to change of L^* in Figure 3. They are relatively small and compensating in the spring but term1 is the largest contribution to the forcing of L^* in the late autumn when λ_c is still close to 0, see Figure 2. The negative L^* in spring, is largely from the lag, i.e., balancing dL_e/dt, whereas in fall its positive values after day 285 are largely contributed by term1, see equation (16).

[46] Figure 4a compares L_e with the 10-year average of L_c, and Figure 4b shows $L^* = L_c - L_e$. The magnitude of L^* is much larger both during the spring ramp-up and fall ramp-down than for the rest of the year, switching to exponential growth and then decay at these times because of the strong dependence of λ on T. Thus the updating of the model L from observations is a most pressing need at these times, and more generally at times of phenological change since these can vary by several weeks from year to year. Equations (12)–(16) effectively represent the contributions of various forms of variability to the climatology of L. We found in comparison to the more exact estimate that equation (14) gives substantial error for the parameters assumed in the example as expected from the large L^* values shown in Figure 4, but that equation (16) was a fairly accurate approximation.

5. Discussion of the Modeling Approach and Its Parameter Dependences

[47] The modeling approach analyzed here represents the observed phenological behavior of leaves in terms of as
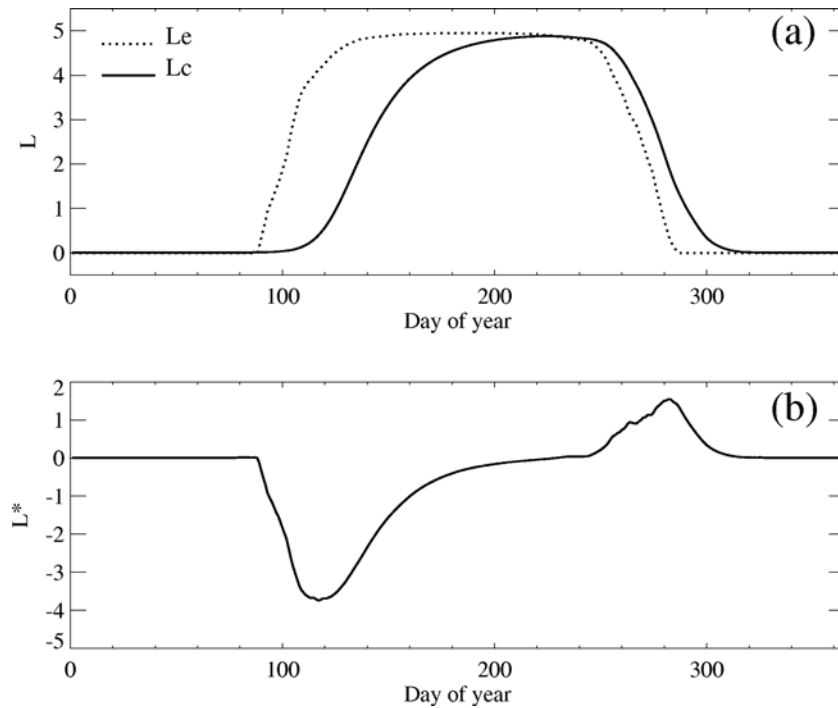
Figure 4. The annual cycle of (a) the ensemble average of $L(=L_c)$ and its equilibrium value L_e and (b) $L^* = L_c - L_e$.

parsimonious as possible a set of parameters and with a model structure that mimics directly the net effect of processes that give this observed behavior. Illustrative calculations of the model dynamics are done with a cold temperature stress term but the framework is intended to also handle water stress terms.

[48] The model structure consists of temperature ramp functions for the turn-off of leaf-loss by cold stress, and a turn-on of growing season leaf-area development. A similar but leaf-area-dependent factor expresses the limit to growth from light saturation. The temperature ramp functions have as parameters, a central temperature and a temperature width. Since cold stress and initial leaf development are totally different biological processes, it is unlikely that these two processes would appear to be at all similar in their temperature dependence. However, any more detailed shape parameters than assumed here may not be resolvable from available data, so for reasons of parsimony we assume the same shape for both processes.

[49] The degree to which light saturation occurs for a given L is controlled by the parameter c that we set to 1, again to limit the number of adjustable parameters. This value has commonly been used by other authors [e.g., *Zeng et al.*, 2005]. The logistic shape of the dependence of λ on L is used primarily because of its simplicity and the judgment that data would not be adequate to distinguish between different choices of such a function.

[50] The model parameters that determine the climatological statistics of the. seasonal trajectories, are controlled by 2 amplitudes, the seasonal minimum and maximum, and two timings, the onset of leaf development and leaf senescence. The model as designed has minimum leaf areas of (near) zero, and maximum values that are controlled by and nearly the same as L_0. The initiation of leaf growth is controlled by the normalized temperature x, the implicit equation $R(x) = (1 + a)/(L_0 + a)$, and hence by the value of a and the two parameters relating x to T giving the temperature which initiates growth. Also affecting the initial appearance of leaf growth and hence the time to its 25% level is the bud/photosynthate forcing term ε, or equivalently some nonzero starting value of L. How fast the leaves then grow and mature depends primarily on their initial exponential growth rate that approaches $\lambda_0 (L_0 - 1)$ ($\sim (5 \text{ day})^{-1}$) as $R(x) \to 1$. However, this rate has little effect on the autumn reduction of leaf area, whose initiation is controlled by the same temperature related parameters as the spring onset and whose loss rate then asymptotes to $(\lambda_0 a)$ ($\sim (2 \text{ day})^{-1}$). Thus the ratio of the time scales for leaf out to leaf drop is approximately $[a/(L_0 - 1)](=9/4)$, i.e., the leaf out period is approximately double the length of the leaf drop period for the parameters used here.

[51] Although the parameter a controls the leaf loss rate for cold temperatures in both autumn and spring (and for which it could use different parameter values), its role in autumn is much more dominant. Except for its implementation with sudden cold snaps, its role in spring can be compensated by the parameters of the temperature-dependent ramp-up function. Another rate simplification choice that has been made is to ignore warm season temperature dependences of the growth and decay rates. We could have included simplified aspects of the temperature dependence of the Farquhar photosynthesis model [e.g., *Dickinson et al.*, 1998] in the growth rate and "Q10" respiration (i.e., the parameter λ_0). However, such dependences would only affect the leaf trajectory somewhat during the growth phase, but are subsumed in the specification of L_0 over the summer season of maximum leaf area.

[52] The model can be extended to allow for additional "slow" variability by an introduction of additional state variables. Previous authors have utilized several assumptions for doing such. For example, the IBIS model, *Foley et al.* [1996] adjusts the maximum leaf area from year to year according to the annual net productivity. *Wei et al.* [2006], on the other hand, use an equation for potential leaf area that is driven by interaction with soil moisture and the actual leaf area. Cold tolerance can also be modeled as a state variable [e.g., *Leinonen et al.*, 1995]. Many other process state variables, e.g., various components of vegetation such as roots or stems, or involving nutrient or carbon cycles [e.g., *Dickinson et al.*, 2002] can be added and would be needed if the parameters of equation (4) are to be adjusted with annual productivity.

[53] Latitudinal and seasonal controls on phenology not explained by temperature are commonly correlated to "photo-period" [e.g., *Jolly et al.*, 2005]. Outside the tropics, such control is largely indistinguishable from daily PAR, which appears to be important in the tropics [e.g., *Myneni et al.*, 2007]. A daily PAR control could be an additional source of climate variability.

6. Conclusions

[54] Dynamic vegetation, as a component of a meteorological prediction model, should include the coupling of thermal and hydrological inputs from the meteorological model, and vary on the shorter time scales of phenological development. The nature of such coupling is illustrated through a toy model that relates leaf-area to scalar measures of temperature and water stress, and illustrative details of this toy model are analyzed for the example of temperature stress.

[55] The toy model for leaf-area is forced by temperature with seasonal, diurnal, and stochastic components. This temperature forcing would likely be related to the canopy and soil temperatures of a meteorological model, but for illustrative purposes, it is generated by a large ensemble of stochastic simulations that mimic statistics of data from a meteorological station. The model remains at its stable equilibrium point of no leaves during the cold season but undergoes unstable growth with warming spring temperatures until it achieves a stable summer equilibrium. The resulting pdfs of the leaf-area are non-Gaussian and nonstationary, with most of their variability concentrated in spring and fall at the times of maximum growth and loss. What determines a climatological leaf-area is analyzed in terms of the statistics of the dynamical model. It is shown to be contributed to by an equilibrium term, a transient term, and various terms determined by correlation statistics, i.e., terms proportional to the variance over the ensemble of the leaf-area and the cyclo-stationary variation of the variance.

[56] Some version of the model of dynamic vegetation described here, if coupled to an adequate canopy radiation model, can be used to provide forward simulations of satellite observed radiances and so should be useful for data assimilation applications.

References

Ahl, D. E., S. T. Gower, S. N. Burrows, N. V. Shabanov, R. B. Myneni, and Y. Knyazikhin (2006), Monitoring spring canopy phenology of a deciduous broadleaf forest using MODIS, *Remote Sens. Environ.*, 104, 88–95.

Arora, V. K., and G. J. Boer (2005), A parameterization of leaf phenology for the terrestrial ecosystem component of climate models, *Global Change Biol.*, 11, 39–59.

Arora, V. K., and G. J. Boer (2006), Simulating competition and coexistence between plant functional types in a dynamic vegetation model, *Earth Interact.*, 10.

Bonan, G. B., S. Levis, S. Sitch, M. Vertenstein, and K. W. Oleson (2003), A dynamic global vegetation model for use with climate models: Concepts and description of simulated vegetation dynamics, *Global Change Biol.*, 9, 1543–1566.

Botta, A., N. Viovy, P. Ciais, P. Friedlingstein, and P. Monfray (2000), A global prognostic scheme of leaf onset using satellite data, *Global Change Biol.*, 6, 709–725, doi:10.1046/j.1365-2486.2000.00362.x.

Chuine, I. (2000), A unified model for budburst of trees, *J. Theor. Biol.*, 207, 337–347.

DeFries, R. S., J. R. G. Townshend, and M. C. Hansen (1999), Continuous fields of vegetation characteristics at the global scale at 1-km resolution, *J. Geophys. Res.*, 104, 16,911–16,923.

Dickinson, R. E., M. Shaikh, L. Graumlich, and R. Bryant (1998), Interactive canopies for a climate model, *J. Clim.*, 11, 2823–2836.

Dickinson, R. E., et al. (2002), Nitrogen controls on climate model evapotranspiration, *J. Clim.*, 15, 278–295.

Ewald, B., C. Penland, and R. Temam (2004), Accurate integration of stochastic climate models with application to El Nino, *Mon. Weather Rev.*, 132, 154–164.

Fisher, J. I., A. D. Richardson, and J. F. Mustard (2007), Phenology model from surface meteorology does not capture satellite-based greenup estimations, *Global Change Biol.*, 13, 707–721.

Fitzjarrald, D. R., O. C. Acevedo, and K. E. Moore (2001), Climatic consequences of leaf presence in the eastern United States, *J. Clim.*, 14, 598–614.

Foley, J. A., I. C. Prentice, N. Ramankutty, S. Levis, D. Pollard, S. Sitch, and A. Haxeltine (1996), An integrated biosphere model of land surface processes, terrestrial carbon balance, and vegetation dynamics, *Global Biogeochem. Cycles*, 10, 603–628.

Foley, J. A., S. Levis, I. C. Prentice, D. Pollard, and S. L. Thompson (1998), Coupling dynamic models of climate and vegetation, *Global Change Biol.*, 4, 561–579.

Friedl, M. A., et al. (2002), Global land cover mapping from MODIS: Algorithms and early results, *Remote Sens. Environ.*, 83, 287–302.

Friend, A. D., and N. Y. Kiang (2005), Land surface model development for the GISS GCM: Effects of improved canopy physiology on simulated climate, *J. Clim.*, 18, 2883–2902, doi:10.1175/JCLI3425.1.

Fung, I., S. C. Doney, K. Lindsay, and J. John (2005), Evolution of carbon sinks in a changing climate, *Proc. Natl. Acad. Sci. U.S.A.*, 102, 11,201–11,206.

Hunter, A. F., and M. J. Lechowicz (1992), Predicting the timing of budburst in temperate trees, *J. Appl. Ecol.*, 29, 597–604.

Jolly, W. M., and S. W. Running (2004), Effects of precipitation and soil water potential on drought deciduous phenology in the Kalahari, *Global Change Biol.*, 10, 303–308, doi:10.1046/j.1529-8817.2003.00701.x.

Jolly, W. M., R. Nemani, and S. W. Running (2005), A generalized, bioclimatic index to predict foliar phenology in response to climate, *Global Change Biol.*, 11, 619–632, doi:10.11111/j.1365-2486.2005.00930.x.

Justice, C. O., J. R. G. Townshend, B. N. Holben, and C. J. Tucker (1985), Analysis of the phenology of global vegetation using meteorological satellite data, *Int. J. Remote Sens.*, 6, 1271–1318.

Kaduk, J., and M. Heimann (1996), A prognostic phenology scheme for global terrestrial carbon cycle models, *Clim. Res.*, 6, 1–19.

Kathuroju, N., M. A. White, J. Symanzik, M. D. Schwartz, J. A. Powell, and R. R. Nemani (2007), On the use of the Advanced Very High Resolution Radiometer for development of prognostic land surface phenology models, *Ecol. Modell.*, 201, 144–156.

Kim, Y., and G. L. Wang (2005), Modeling seasonal vegetation variation and its validation against Moderate Resolution Imaging Spectroradiometer (MODIS) observations over North America, *J. Geophys. Res.*, 110, D04106, doi:10.1029/2004JD005436.

Knyazikhin, Y., J. V. Martonchik, R. B. Myneni, D. J. Diner, and S. W. Running (1998), Synergistic algorithm for estimating vegetation canopy leaf area index and fraction of absorbed photosynthetically active radiation from MODIS and MISR data, *J. Geophys. Res.*, 103, 32257–32274.

Koetz, B., F. Baret, H. Poilve, and J. Hill (2005), Use of coupled canopy structure dynamic and radiative transfer models to estimate biophysical canopy characteristics, *Remote Sens. Environ.*, 95, 115–124.

Kucharik, C. J., C. Barford, M. El Maayar, S. C. Wofsy, R. K. Monson, and D. D. Baldocchi (2006), A multiyear evaluation of a dynamic global vegetation model at three AmeriFlux forest sites: Vegetation structure, phenology, soil temperature, and CO2 and H2O vapor exchange, *Ecol. Modell.*, *196*, 1–31.

Leinonen, I., T. Repo, H. Hanninen, and K. E. Burr (1995), A second-order dynamic model for the frost hardiness of trees, *Ann. Bot.*, *76*, 89–95.

Leinonen, I. (1996), A simulation model for the annual frost hardiness and freeze damage of Scots pine, *Ann. Bot.*, *78*, 687–693.

Levis, S., and G. B. Bonan (2004), Simulating springtime temperature patterns in the Community Atmosphere Model coupled to Community Land Model using prognostic leaf area, *J. Clim.*, *17*, 4531–4540, doi:10.1175/3218.1.

Liu, Q., L. Gu, R. E. Dickinson, Y. Tian, L. Zhou, and W. M. Post (2008), Assimilation of satellite reflectance data into a dynamical leaf model to infer seasonally varying leaf area for climate and carbon models, *J. Geophys. Res.*, doi:10.1029/2007JD009645, in press.

Moody, E. G., M. D. King, S. Platnick, C. B. Schaaf, and F. Gao (2005), Spatially complete global spectral surface albedos: Value-added datasets derived from Terra MODIS land products, *IEEE Trans. Geosci. Remote Sens.*, *43*, 144–158.

Myneni, R. B., et al. (2007), Large seasonal changes in leaf area of amazon rainforests, *Proc. Natl. Acad. Sci.*, *102*, 4820–4823.

Prentice, I. C., W. Cramer, S. P. Harrison, R. Leemans, R. A. Monserud, and A. M. Solomon (1992), A global biome model based on plant physiology and dominance, soil properties and climate, *J. Biogeogr.*, *19*, 117–134.

Richardson, A. D., A. S. Bailey, E. G. Denny, C. W. Martin, and J. O'Keefe (2006), Phenology of a northern hardwood forest canopy, *Global Change Biol.*, *12*, 1174–1188.

Schaaf, C. B., et al. (2002), First operational BRDF, albedo, and nadir reflectance products from MODIS, *Remote Sens. Environ.*, *83*, 135–148.

Shukla, J., and J. L. Kinter III (2006), Predictability of seasonal climate variations: A pedagogical review, pp. 306–341, in *Predictability of Weather and Climate*, edited by T. Palmer and R. Hagedorn. 702 pp., Cambridge Univ. Press, Cambridge, UK.

Wei, J., R. E. Dickinson, and N. Zeng (2006), Climate variability in a simple model of warm climate land-atmosphere interaction, *J. Geophys. Res.*, *111*, G03009, doi:10.1029/2005JG000096.

White, M. A., P. E. Thornton, and S. W. Running (1997), A continental phenology model for monitoring vegetation responses to interannual climatic variability, *Global Biogeochem. Cycles*, *11*, 217–234.

White, M. A., and R. R. Nemani (2006), Real-time monitoring and short-term forecasting of land surface phenology, *Remote Sens. Environ.*, *104*, 43–49, doi:10.1016/j.rse.2006.04.014.

Williams, C. N., Jr., M. J. Menne, R. S. Vose, and D. R. Easterling (2006), United States Historical Climatology Network Daily Temperature, Precipitation, and Snow Data, ORNL/CDIAC-118, NDP-070. Available on-line [http://cdiac.ornl.gov/epubs/ndp/ushcn/usa.html] from the Carbon Dioxide Information Analysis Center, Oak Ridge National Laboratory, U.S. Department of Energy, Oak Ridge, Tenn.

Yan, W., and D. H. Wallace (1998), Simulation and prediction of plant phenology for five crops based on photoperiod × temperature interaction, *Ann. Bot.*, *81*(6), 705–716.

Zeng, X. D., X. Zeng, S. S. P. Shen, R. E. Dickinson, and Q.-C. Zeng (2005), Vegetation-soil water interaction within a dynamical ecosystem model of grassland in semi-arid areas, *Tellus*, *57B*, 189–202.

Zhang, X., M. A. Friedl, C. B. Schaaf, A. H. Strahler, J. C. F. Hodges, F. Gao, B. C. Reed, and A. Huete (2003), Monitoring vegetation phenology using MODIS, *Remote Sens. Environ.*, *84*, 471–475.

Zhang, X., M. A. Friedl, C. B. Schaaf, and A. H. Strahler (2004), Climate controls on vegetation phenological patterns in northern mid- and high latitudes inferred from MODIS data, *Global Change Biol.*, *10*, 1133–1145, doi:10.1111/j.1365-2486.2004.00784.x.

Zhang, X., M. A. Friedl, C. B. Schaaf, A. H. Strahler, and Z. Liu (2005), Monitoring the response of vegetation phenology to precipitation in Africa by coupling MODIS and TRMM instruments, *J. Geophys. Res.*, *110*, D12103, doi:10.1029/2004JD005263.

————————————

R. E. Dickinson, Q. Liu, and L. Zhou, School of Earth and Atmospheric Sciences, Georgia Institute of Technology, 311 Ferst Drive, Atlanta, GA 30332-0340, USA. (robted@eas.gatech.edu)

Y. Tian, IMSG at NOAA NEDIS, 5200 Auth Road, Camp Springs, MD 20746, USA.